Received: 7 July 2023 | Revised: 15 September 2023 | Accepted: 30 September 2023

DOI: 10.1111/jtxs.12806

RESEARCH ARTICLE

Journal of Texture Studies WILEY

Quantitative characterizations of visual fibrousness in meat analogues using automated image analysis

Yizhou Ma | Miek Schlangen | Jelle Potappel | Lu Zhang | Atze Jan van der Goot

Laboratory of Food Process Engineering, Wageningen University, Wageningen, The Netherlands

Correspondence
Atze Jan van der Goot, Laboratory of Food Process Engineering, Wageningen University, PO Box 17, AA, Wageningen 6700, The Netherlands.
Email: atzejan.vandergoot@wur.nl

Funding information
Sectorplan Techniek Mechanical Engineering (NWO)

Abstract

A desirable quality of plant-based meat analogues is to resemble the fibrous structure of cooked muscle meat. While texture analysis can characterize fibrous structures mechanically, assessment of visual fibrous structures remains subjective. Quantitative assessment of visual fibrous structures of meat analogues relies on expert knowledge, is resource-intensive, and time-consuming. In this study, a novel image-based method (Fiberlyzer) is developed to provide automated, quantitative, and standardized assessment of visual fibrousness of meat analogues. The Fiberlyzer method segments fibrous regions from 2D images and extracts fiber shape features to characterize the fibrous structure of meat analogues made from mung bean, soy, and pea protein. The computed fiber scores (the ratio between fiber length and width) demonstrate a strong correlation with expert panel evaluations, particularly on a per-formulation basis ($r^2 = 0.93$). Additionally, the Fiberlyzer method generates fiber shape features including fiber score, fiber area, and the number of fiber branches, facilitating comparisons of structural similarity between meat analogue samples and cooked chicken meat as a benchmark. With a simple measurement setup and user-friendly interface, the Fiberlyzer method can become a standard tool integrated into formulation development, quality control, and production routines of plant-based meat analogue. This method offers rapid, cheap, and standardized quantification of visual fibrousness, minimizing the need for expert knowledge in the process of quality control.

KEYWORDS
fibrous structure, image analysis, meat analogues, quality control, rapid method

1 | INTRODUCTION

Sustainability, health, and animal welfare concerns have motivated consumers to replace their dietary protein sources from animals to plants, boosting the demand for plant-based meat analogues (McClements & Grossmann, 2022). As alternatives, meat analogues have the highest success rate when they deliver a sensory experience similar to the experience of consuming meat (Michel et al., 2021). Texture, in particular a fibrous structure, is one of the most defining quality attributes of meat analogues for consumer

Yizhou Ma and Miek Schlangen should be considered joint first authors.

acceptability (Elzerman et al., 2011). A fibrous and muscle meat-like texture can be produced through thermomechanical processing of plant proteins by, for example, high moisture extrusion (HME) cooking, low moisture extrusion (LME) cooking, or high temperature shear cell (HTSC) technology (Dekkers et al., 2018; Grabowska et al., 2014; Kyriakopoulou et al., 2019; McClements & Grossmann, 2022; Webb et al., 2023). In recent years, LME, HME cooking, and HTSC technology have produced meat analogues with a range of different structures containing various plant protein compositions (Kyriakopoulou et al., 2019; McClements & Grossmann, 2022; Webb et al., 2023).

To better compare between samples, fibrous structures of meat analogues are often characterized by mechanical, spectral, and imaging techniques (Mcclements et al., 2021; Schreuders, Schlangen, Kyriakopoulou, Boom, & van der Goot, 2021). Mechanical anisotropy, measured through tensile testing, is generally used to describe fibrous structures of HTSC products, but does not always agree with visual observations of macrostructure (Barbut, 2015; Schreuders, Schlangen, Bodnár, et al., 2021). Only weak correlations were found between consumer visual assessment of fibrous structures and mechanical attributes in meat analogues (Godschalk-Broers et al., 2022). Thus, it remains uncertain whether fibrous structures of meat analogues can be fully characterized by mechanical anisotropy. Hence, relying solely on the mechanical anisotropy of meat analogues may not be sufficient to assess their textural quality. Spectral techniques, such as fluorescence polarization and light reflectance, can also indirectly characterize visual fibrousness of meat analogues. The fiber orientations (i.e., anisotropic structures) create unique light reflectance and fluorescence polarization patterns, which can be used to measure fibrous structures of meat analogues (Ranasinghesagara et al., 2006, 2009). However, such spectral methods require special instrumentations and algorithm development, which complicates the general use of this visual fibrousness characterization process. In practice, many studies relied on manual inspections of the fibrous structures of meat analogues (Dekkers et al., 2016; Grabowska et al., 2014, 2016; Jia et al., 2021; Krintiras et al., 2015; Osen et al., 2014; Schreuders et al., 2019). While reporting images of inner structures is a simple and effective way to compare the visual fibrousness of meat analogues, it limits the results to subjective and qualitative interpretations. A robust and quantitative measurement of visual fibrousness of meat analogues can provide objective characterization of fiber formation across different formulations and processing parameters, making subjective human evaluations less important. Furthermore, with an automated and quantitative measurement of fibrousness, it can monitor the production of meat analogues and provide feedback for structuring improvement.

A promising technique for developing such a method is computer vision (CV). CV is a collection of algorithms that allow digital interpretation of visual information from images and videos. CV has been widely used in agri-food applications, such as in meat analogue color analysis, 3D food printing performance, and meat quality evaluation (Fan et al., 2013; Ma, Potappel, Chauhan, et al., 2023; Taheri-Garavand et al., 2019). Furthermore, one study applied a CV algorithm, called Hough transformation, to calculate a fiber index for a set ($n = 9$) of meat analogues produced through HME cooking (Ranasinghesagara et al., 2005). The study found that fiber index calculated from image analysis correlated well with a noninvasive fluorescence polarization method. However, as Hough transformation only detects straight lines on an image, the method developed by Ranasinghesagara et al. (2005) may have limitations when detecting inner structures with curved or bended fibers as for example found in HTSC samples. Other CV techniques such as shape analysis have been applied to provide comprehensive morphological characterizations of barley kernels and wheat grains (Sharma et al., 2021; Zapotoczny et al., 2008). These morphological analysis methods can potentially be adopted to measure the visual fibrousness of meat analogues. Furthermore, while the conventional evaluations by human experts can only provide a single value to assess fibrousness, a CV-based method has the potential to offer visual similarity assessment, for example using real meat, because it can characterize multiple morphological features of the fibrous structures. A first step in the development of this tool is the validation of the quantitative measure of fibrous structure with a CV-based method and to place it into context with human evaluations, which can then establish practical significance of an automated method (Ma, Potappel, Schutyser, et al., 2023). Eventually, such tool could replace time- and resource-consuming human evaluations for the quality control of meat analogues.

This study aims to develop an automated visual assessment method called "Fiberlyzer" based on CV to quantify fibrousness of meat analogues. Specifically, the Fiberlyzer method utilizes image segmentation followed by shape analysis to calculate a robust fiber score to serve as an alternative to human evaluation. The computed fiber score is then validated by expert fiber scores collected from a survey. Additionally, the method generates a unique texture fingerprint for each image, allowing precise comparison between texture of meat and meat analogues.

2 | MATERIALS AND METHODS

2.1 | Materials

Soy protein isolate (SPI) (Supro 500E), pea protein isolate (PPI) (NUTRALYS® F85M), and mung bean protein isolate (MBPI) (UNIMUNG M70) were obtained from Solae (Dupont, St. Louis, MO, USA), Roquette Freres S.A. (St. Louis, Missouri, USA), and Barentz (Hoofddorp, NL), respectively. SPI, PPI, and MBPI were composed of 81.7 wt.% ($N \times 5.7$), 74.5 wt.% ($N \times 5.4$), and 68.9 wt.% ($N \times 5.7$) protein on a dry weight basis using a rapid N exceed® analyzer (Elementar, Langenselbold, Germany). SPI, PPI, and MBPI had a dry matter content of 91.2, 92.4, and 97.3 wt.%, respectively. Cooked chicken breast (Scharrel Kipfilet, Albert Heijn, the Netherlands), tofu (Biologische tofu naturel, Albert Heijn, the Netherlands), and vegan chicken (De Vegetarische Slager Kipstuckjes, Unilever, the Netherlands) were purchased at a local supermarket (Albert Heijn, the Netherlands).

2.2 | Sample preparation

To obtain meat analogue samples with a variety of textures, plant proteins were structured using the HTSC technology (Wageningen University & Research, the Netherlands). First, protein doughs were prepared by manually mixing various amounts of demineralized water with SPI, PPI, or MBPI to achieve final dry matter concentrations of 35, 40, or 45 wt.% (Table 1). In addition, blended protein doughs were made by combining SPI and PPI or SPI and MBPI in a 50:50 ratio (Table 1). Formulations made from MBPI and SPI with 45 wt.% dry matter are missing, as these could not be structured into meat analogues in preliminary experiments due to poor protein hydration. In total, 13 formulations were prepared for subsequent shear cell structuring.

The protein doughs were covered with parafilm and left to hydrate at room temperature (20°C) for 30 min. The doughs were then loaded into a pre-heated HTSC to structure them into meat analogues. During the HTSC process, the materials were sheared at a rate of 39 s^{-1}, 120°C for 15 min (controlled by a Haake Polylab QC drive, Germany). Subsequently, the samples were cooled at 0 s^{-1} for 5 min, using an external oil bath with a temperature of 25°C. The cooled sample was removed from the HTSC, tempered to room temperature, sealed in an air-tight bag, and stored in the freezer (−18°C) until further analysis. Freezing can positively impact the fibrous appearance and has previously been applied to texturize animal and fish proteins and soy protein gels (Chantanuson et al., 2022; Dekkers et al., 2018).

2.3 | Image acquisition and pre-processing

The frozen HTSC sample was first thawed to 20°C, and three squares of approximately 3 × 3 cm were randomly cut out and manually folded open in the direction parallel to the shear flow to expose the inner structure. The folded sample was held in place by a clamp and imaged in a light-controlled photo booth with a digital camera (A6000, SONY, Japan) equipped with a 100 mm macro lens (Tokina, Tokyo, Japan). The camera was placed approximately 20 cm from the folded sample. Figure 1a,b provide an example image of the inner structure of the HTSC sample. After obtaining the raw images, a region of interest was manually selected by cropping out the background to allow assessment of the inner structure of the HTSC samples (Figure 1c). For samples that were completely fractured (i.e., Figure 1b), region of interest was only focussed on half of the sample to avoid fracture edges (Figure 1d).

2.4 | Expert visual assessment of fibrous structures

Quantitative visual assessment was performed through an online survey designed in Qualtrics (Washington, USA). Twenty-six experts with prior experience in evaluating macrostructures of HTSC meat analogues were recruited for this study. The survey consisted of 13 images of HTSC meat analogues, three images of commercial samples (cooked chicken breast, tofu, and vegan chicken), and two mirrored images as quality control samples. The two mirrored images were included to check whether the experts rated products with identical fibrousness similarly. All images were acquired and pre-processed as described in Section 2.3.

Experts were instructed to evaluate fibrousness of the samples on a visual analogue slider ranging from 0 to 100. The slider contained five labels (not fibrous, somewhat fibrous, fibrous, very fibrous, and extremely fibrous) at the 0, 25, 50, 75, and 100 positions. Furthermore, images of a nonfibrous and an extremely fibrous HTSC sample served as references and were presented to the experts at the beginning of each survey question. For every HTSC and commercial sample, one out of five images was randomly selected and presented to an expert. With 26 experts, this resulted in at least five evaluations per image. The median of the five scores was calculated and used as a measure for expert visual fibrousness. All experts were presented the same mirrored images to evaluate the consistency in fibrousness evaluations. A sample survey is available in the Supplementary Materials of this study.

TABLE 1 Overview of the dry matter composition of the doughs prepared from mung bean protein isolate (MBPI), pea protein isolate (PPI), soy protein isolate (SPI), and combinations of SPI-MBPI and SPI-PPI.

Protein ingredient(s)	MBPI (wt.%)	PPI (wt.%)	SPI (wt.%)	Total dry matter (wt.%)
MBPI	35	–	–	35
	40	–	–	40
PPI	–	35	–	35
	–	40	–	40
	–	45	–	45
SPI	–	–	35	35
	–	–	40	40
SPI-MBPI	17.5	–	17.5	35
	20	–	20	40
	22.5	–	22.5	45
SPI-PPI	–	17.5	17.5	35
	–	20	20	40
	–	22.5	22.5	45

2.5 | Fiberlyzer: Automated visual assessment of fibrous structures

Fiberlyzer, a Python-based image analysis method, was developed to automate the visual assessment of fibrous structures of the HTSC meat analogue samples. The automated visual assessment pipeline consisted of image collection, segmentation, and shape analysis (Figure 2). The image collection and pre-processing step was introduced in Section 2.3, and the details of segmentation and shape analysis steps are introduced in the following sections.

2.5.1 | Segmentation of fibrous regions

To automatically identify the fibrous regions of an inner structure, a segmentation method is required. The saturation values of color images have shown correlations to 3D shape perceptions in the human visual system (Marlow et al., 2022). Therefore, a saturation-based technique was used to identify and segment potentially fibrous regions on the pre-processed image. The images were first converted into the hue, saturation, value color space, and a threshold level was set to create a binary image. The binary image was smoothed using the Gaussian pyramid construction and median blur with a filter size of 7×7 pixels. Connected component analysis was then performed to identify and locate the individual fibrous regions using a connectivity of four. A minimal area of a connected component was defined as a fraction of the total image size and used to filter unwanted noise from the prior binarization step.

2.5.2 | Fiber shape analysis

Each isolated region was then analyzed separately to obtain various shape features. For each region, image skeletonization was used to identify a set of curves that pass through the center of connected regions known as the "skeleton." The longest path (L_{max}) was found by iteratively looping through all unique pairs of branches of the skeleton. Meanwhile, the Euclidean distance (L_E) between the start and

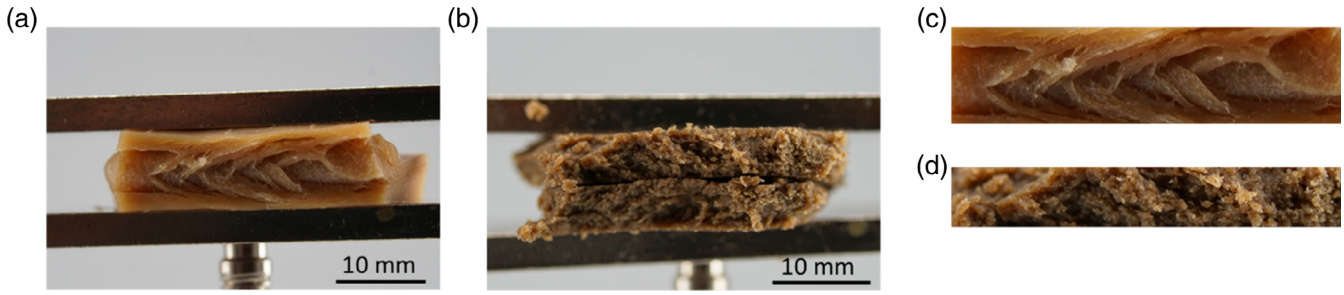

FIGURE 1 Example images of samples produced for this study. (a) An image of a folded sample made of soy protein isolate (35%). (b) An image of a folded sample made of mung bean protein isolate (35%). (c) The cropped image of soy protein isolate sample shown in (a). (d) The cropped image of mung bean protein isolate sample shown in (b).

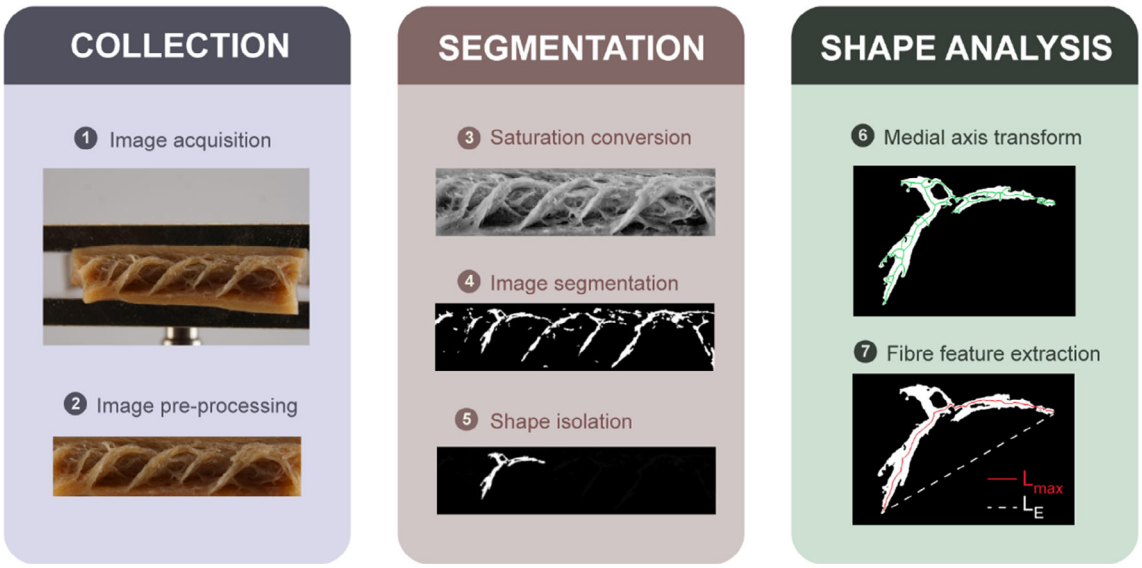

FIGURE 2 Fiberlyzer workflow consisting of collection, segmentation, and shape analysis. L_{max} indicates longest skeleton path. L_E indicates Euclidian distance between start and end points of the longest path.

end points of the longest path was calculated, and a curvature factor was then determined by taking the ratio between L_{max} and L_E. Only regions with a curvature factor of less than 1.2 were further analyzed to avoid over-curved skeletons. The shortest distance from each pixel on a skeleton to the edge of the shape was then calculated for each isolated skeleton. These distances were averaged to obtain the width of the potential fibrous region. Image skeletonization was then performed on all isolated regions to obtain the length, width, area, and number of branches of the individual region. A fiber score, F, was calculated for each region with Equation 1.

$$F = \frac{\text{longest skeleton path length}}{\text{average path width}}. \quad (1)$$

The average fiber score, $\overline{F}$, was calculated among all isolated regions of one image and served as the main shape feature to quantify fibrousness of the meat analogue sample. To obtain the best segmentation parameters, a grid search was performed using a range of minimal area (from 0.005% to 0.05%) and saturation threshold (from 80% to 95%) to calculate $\overline{F}$ of each image.

2.6 | Visual fiber similarity analysis

While the computed fiber score from Fiberlyzer gives a quantitative fibrousness assessment at the image level, additional fiber similarity analysis was carried out to measure how closely the fibrous structure from HTSC samples resembles cooked chicken breast. The obtained fiber shape features of HTSC samples were compared with those obtained from a reference image of cooked chicken breast. Distributions of fiber score, area, and number of branches were overlayed with those from the reference image, respectively. The overlapped area of the two distributions, $f(x)$ for meat analogue samples and $g(x)$ for the reference sample, was estimated by calculating the coefficient of overlapping (Δ) using a method developed by Ridout and Linkie (2009) (Equation 2).

$$\Delta(f,g) = \int \min\{f(x), g(x)\}dx, \quad (2)$$

where x represents the individual shape feature of fiber score, fiber area, or number of fiber branches.

The $\Delta(f,g)$ of each shape feature was then averaged to obtain a collective similarity score between a given HTSC sample and the reference chicken breast.

2.7 | Data analysis and software availability

Pearson's correlation tests were conducted using the R programming language. The Fiberlyzer method was developed in-house using the OpenCV, NumPy, Pandas, and Matplotlib libraries in the Python programming language. The software including a graphical user interface, raw scripts, and raw images used for the software development are open-source and can be accessed through: https://git.wur.nl/yizhou.ma/fiberlyzer3.

3 | RESULTS AND DISCUSSION

In the following sections, the expert assessment of visual fibrousness is first introduced to understand structural differences among the HTSC samples produced in this study. We then highlight the shape feature measurements from the Fiberlyzer method. The aggregated measurement from the Fiberlyzer method was correlated with the expert assessment as a validation. A visual fiber similarity analysis between a reference cooked chicken image and HTSC sample images was also performed to select formulations with the highest potential to mimic chicken. Lastly, we discuss the limitations and future applications of the Fiberlyzer method.

3.1 | Expert assessment of visual fibrousness

Visual fibrousness of meat analogues and commercial products (tofu, vegan chicken, and chicken) were assessed in a survey of 26 meat analogue experts. Quality control samples (mirrored images of a HTSC sample) were included in the survey to check the consistency of the fiber scoring among the experts. No significant difference ($p > .05$) in fiber score was found between the two quality control images ($\mu_{\text{mirrored image}} = 43.1$, $\mu_{\text{non-mirrored image}} = 42.8$), showing that the experts were consistent when assigning fiber scores. However, the expert fiber scores of the quality control samples had a large variation with a range between 0 and 85 (Figure S1). The large scoring variation is likely due to that the experts were untrained to specifically rate fibrousness of HTSC samples, so the fiber scores were not primed toward a certain range or calibrated with standards. Nevertheless, the expert survey revealed differences in fibrousness among the surveyed samples (Figure 3). MBPI 35 and 40 wt.% were found to exhibit no visual fibrousness, with median fiber scores of 0. The fibrousness assessment agrees with previous findings, where pure MBPI-based meat analogues were described as "gel-like" and displayed no fiber formation (Samard & Ryu, 2019; Schlangen et al., 2023). For PPI samples, at 35 and 40 wt.%, very minimal fibrousness was found from the expert survey. In previous studies, PPI was often blended with other ingredients, such as wheat gluten and pectin, to assist structure elongation and form anisotropy (Schreuders et al., 2019; Schreuders, Schlangen, Bodnár, et al., 2021). However, PPI alone has been texturized into a fibrous structure at high dry matter content (45 wt.%) using HME cooking before (Osen et al., 2014). This finding from Osen et al. (2014) agrees with the fiber scores rated by the experts in this study, showing the potential of producing fibrous structures of PPI at high dry matter content (45 wt.%).

SPI samples and SPI-PPI blends both showed higher fiber scores compared to the other HTSC samples (Figure 3). Typically, wheat gluten or pectin is added to SPI to induce fiber formation in shear

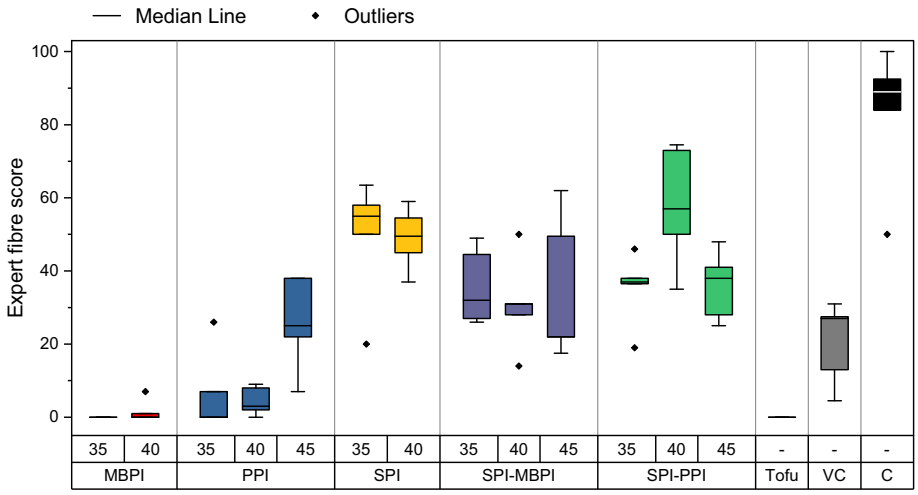

FIGURE 3 Expert fiber scores of high temperature shear cell samples with various dry matter contents (35, 40, and 45 wt.%). C, chicken; MBPI, mung bean protein isolate; PPI, pea protein isolate; SPI, soy protein isolate; VC, vegan chicken.

structuring, as SPI alone was previously shown not to form a fibrous structure (Dekkers et al., 2016). However, freezing may have assisted fiber formation in this study. It is also worth mentioning that the blend of two nongluten proteins (SPI-MBPI and SPI-PPI) could be structured into fibrous products, which was only reported from a previous HME cooking study (Wittek et al., 2021). Overall, the variations in expert fiber scores show that inner structures of HTSC samples exhibit differences. The wide range of expert fiber scores can therefore be used as references for the subsequent validation of the Fiberlyzer method.

3.2 | Fiber shape features in meat analogues

The image-based Fiberlyzer method can provide measurements of fiber shape features including the fiber score, fiber area, and number of fiber branches. For example, Figure 4 highlights distributions of shape features of four images acquired in this study. Figure 4a shows the variation in computed fiber score among cooked chicken, MBPI with 35 wt.% dry matter, SPI-PPI with 35 wt.% dry matter, and tofu images. The chicken image had a bimodal distribution of the computed fiber score with peaks centers around 5 and 17. Such a broad range of fiber scores agreed with the hierarchical fiber presence of cooked chicken (Figure 4a) as meat muscle fibers occur at different length scales (van der Sman & van der Goot, 2023). MBPI with 35 wt.% dry matter had a narrow distribution with a low fiber score peak around 3. The narrow distribution of the fiber score corresponded well with the image of the sample, of which the MBPI 35 wt.% dry matter sample appeared to be crumbly and grainy. On the other hand, the computed fiber score distribution of SPI-PPI with 35 wt.% dry matter was bimodal with a broad distribution of scores, similar to chicken. The fibrousness of the SPI-PPI 35 wt.% dry matter was also scored closer to chicken in the expert evaluation (Figure 3). The similarity in fiber score distribution between chicken and SPI-PPI 35 wt.% dry matter may explain the higher expert fiber score that SPI-PPI 35 wt.% dry matter received (Figure 3). The computed fiber score may therefore be an indication of the expert fiber scores collected from the survey.

However, the tofu image also yielded a computed fiber score distribution that was relatively similar to the HTSC samples (Figure 4a). Nonetheless, the computed fiber distribution of tofu disagreed with the expert panel results in Figure 3, where all experts gave a fiber score of 0 for the tofu image. Tofu may carry a different fractal appearance from HTSC samples upon folding, because of its relatively isotropic structure. Also, the surface moisture on tofu may have interfered with the fiber segmentation algorithm developed in this study. The unexpected high fiber score indicated that tofu was an outlier in visual fibrousness assessment using Fiberlyzer and was therefore discarded for subsequent analysis.

For the area distributions (Figure 4b), MBPI with 35 wt.% dry matter showed a sharp distribution centered around a lower value compared to the broad distribution of chicken. The lower fiber area may correspond to the crumbly and granular texture observed in the image. The small granules were segmented and identified by the Fiberlyzer as small fiber areas. By comparing the area distributions, SPI-PPI with 35 wt.% dry matter had a similar fiber area range as the chicken image, indicating the potential similarity in visual fibrousness. Figure 4c illustrates distributions of number of fiber branches identified in the samples. Again, the SPI-PPI sample with 35 wt.% dry matter appeared to have a more similar distribution to chicken than the MBPI with 35 wt.% dry matter. The distinct fiber shape features of different samples showed the potential of using the Fiberlyzer method to characterize fibrous structures of HTSC samples.

3.3 | Validation of computed fiber scores

Although fiber shape feature distributions can characterize the fibrous structures of HTSC samples, further analysis is needed to directly compare the computed fiber shape features to the expert fiber scores. The fiber shape features were averaged per image to produce aggregated representations of fiber score, fiber area, and the number of fiber branches. Because segmentation parameters during image analysis can impact the shape feature calculation, a grid search was

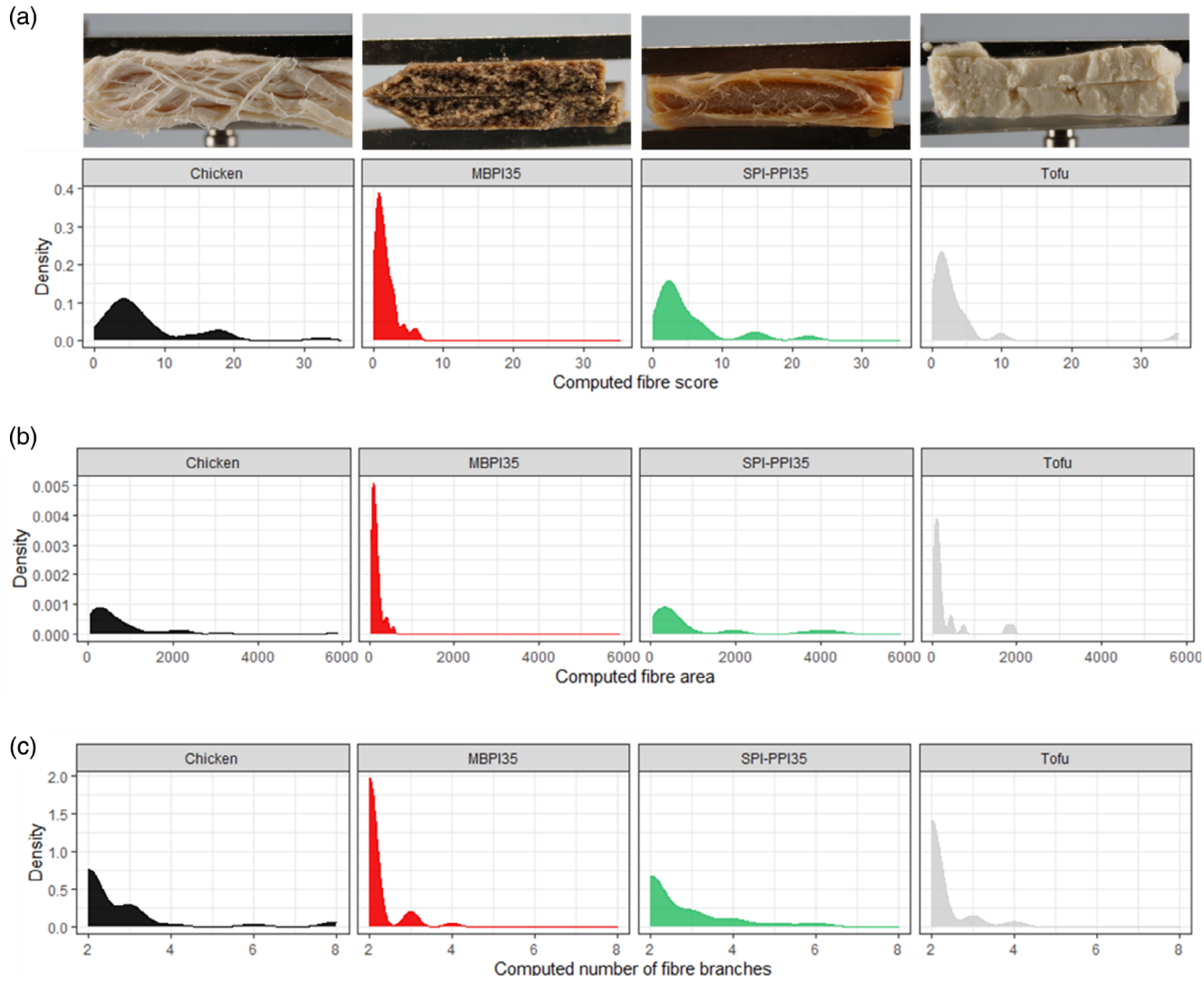

FIGURE 4 Example measurements of fiber shape features of chicken, mung bean protein isolate (35 wt.%) (MBPI35), a blend of soy protein isolate and pea protein isolate (35 wt.%) (SPI-PPI35), and tofu. (a) Distributions of computed fiber score. (b) Distributions of computed fiber area. (c) Distribution of number of fiber branches.

performed to identify the best combination of segmentation parameters. The correlation of determination (r^2) was used as the parameter selection criterion when determining the segmentation parameters of threshold percentile and minimal fiber area. During preliminary experiments, we only found significant correlations between the averaged computed fiber score and the expert fiber score, so the subsequent validation focused on evaluating computed fiber score as an automated measurement to replace expert visual assessment.

The correlation between the computed fiber score and expert fiber score was influenced by both the threshold percentile and the minimal area (Figure 5a). A high threshold percentile reduced the r^2 value, likely due to the exclusion of fibrous regions during the saturation-based segmentation step. Conversely, a low threshold percentile led to an overestimation of fibrous regions, including nonfibrous areas (i.e., noise) falsely identified as region of interests. When the minimal area was set below 0.03%, a decrease in correlation was observed, probably due to the inclusion of relatively small regions (i.e., noise) that are nonfibrous in nature but that were used in the calculation of the computed fiber score. The combination of an 82% threshold percentile and a 0.045% minimal area yielded the highest r^2 value and were thus selected as the best segmentation parameters on a per-image basis. These parameters were used to plot the computed fiber score against the expert fiber score, resulting in a r^2 of 0.66 on a per-image basis (Figure 5c). This moderate correlation suggests that the Fiberlyzer method can partially replace the expert evaluation of visual fibrousness. The computed fiber scores effectively differentiated between the nonfibrous images (MBPI) and highly fibrous images (chicken). However, comparing the other samples remains inconclusive due to the variations in fibrous structure from image to image.

To account for the image-to-image variations, Figure 5b,d present a formulation-based comparison by averaging the scores of

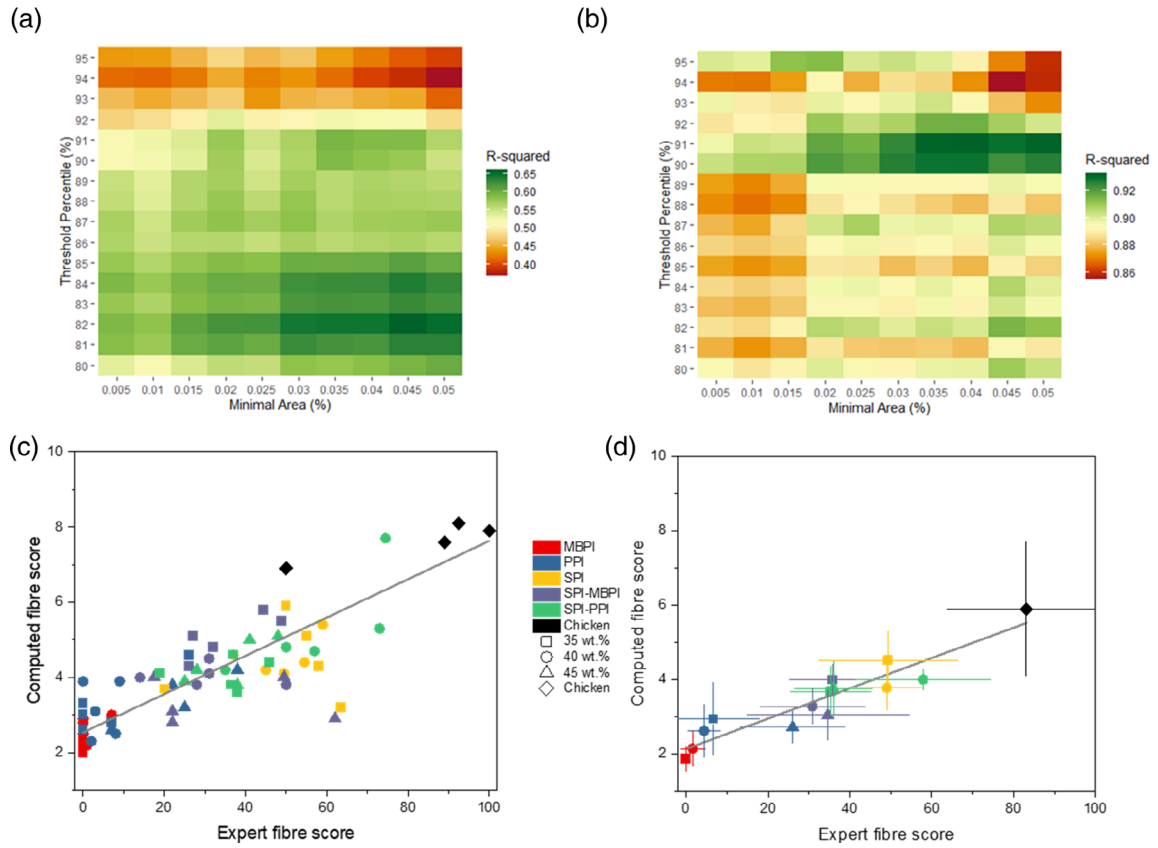

FIGURE 5 Parameter correlation on (a) per-image basis and (b) per-formulation basis, and corresponding scatter plots of expert fiber score versus computed fiber score with (c) threshold percentile of 82% and minimal area of 0.045%, and (d) threshold percentile of 91% and minimal area of 0.04%.

5 images of the same formulation. Here, a higher threshold percentile (91%) and a lower minimal area (0.040%) improved the r^2 to 0.93. From Figure 3 it already became evident that there were considerable variations in the expert fiber scores. Figure 5d reveals large variations in computed fiber score as well. The variations in computed fiber score can be attributed to the inhomogeneous fiber distribution within the meat analogues, which may be a desired property of the product. However, the variations could also be explained by variations in selecting of samples and/or imaging technique. The large inner structure variations were also reported in other studies based on x-ray tomographic characterizations (Nieuwland et al., 2023). Similar to the expert survey results, chicken images scored higher than the meat analogue images, despite variations in computed fiber scores. Overall, the averaged result on a formulation basis improved the correlation ($r^2 = 0.93$), suggesting that the Fiberlyzer is a practical method to replace expert fiber assessment digitally.

3.4 | Image-based similarity analysis

While the computed fiber score provides automated and direct quantification of fibrous structures, it is also important to understand how closely the HTSC samples can mimic the visual appearance of meat products. To quantify the similarity found in the three fiber shape features (fiber score, fiber area, or number of fiber branches), a similarity analysis method (Equation 2) was implemented by considering the distribution overlapping between a HTSC sample image and a reference chicken image (Figure S2). Figure 6a shows the similarity analysis based on overlapping of averaged shape feature distributions. Four other chicken images were used as benchmarks to establish a threshold similarity score. In Figure 6a, the chicken similarity scores ranged from 0.64 to 1, indicating that a "chicken-like" sample should have a similarity score of at least 0.64. Among each formulation, a large variation was found again, due to the structural heterogeneity of the HTSC samples as discussed in Section 3.2. Although with variations, MBPI samples were found to be the most dissimilar to the chicken reference image (Figure 6a). Samples made from other formulations had no clear distinctions when comparing all three shape features to determine similarity. Several samples had a similarity score exceeding the threshold as indicated by the dash line, which suggests resemblance to the reference cooked chicken image according to the Fiberlyzer method. However, similarity score computed based on the average parameters may not provide the required resolution to differentiate fibrous structures among HTSC samples.

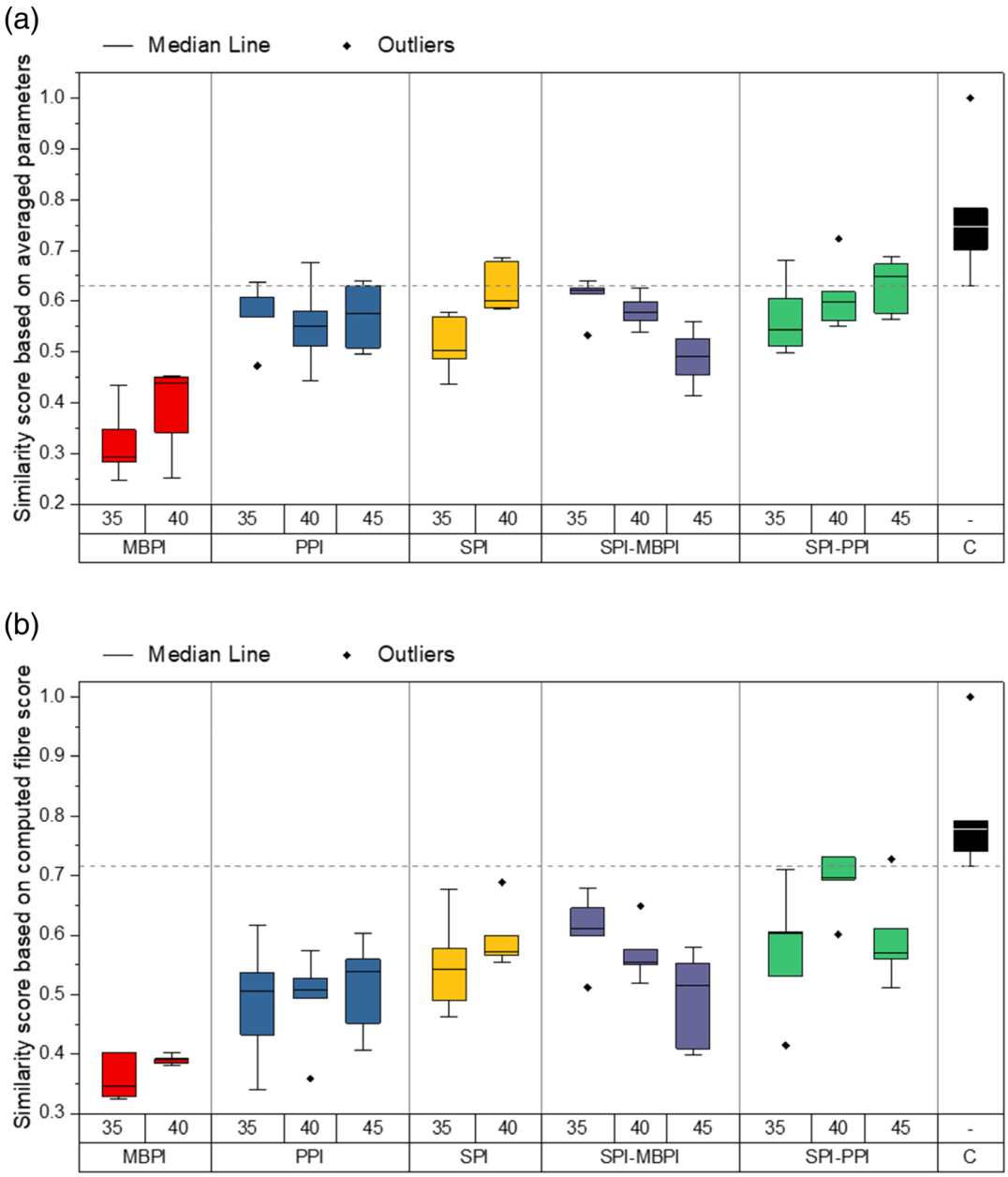

FIGURE 6 Visual similarity analysis between high temperature shear cell samples and cooked chicken based on averaged shape features (a) and computed fiber score (b). MBPI, mung bean protein isolate; PPI, pea protein isolate; SPI, soy protein isolate. (c): cooked chicken. Samples were produced at dry matter contents of 35, 40, and/or 45 wt.%. Dashed line indicates similarity threshold to cooked chicken.

With no clear distinction in fiber similarity based on three shape features, Figure 6b evaluates fiber similarity using the fiber scores alone. A new similarity threshold (0.72) was determined based on the reference chicken images. A large range of similarity (0.35–0.6) was found in the PPI samples, indicating large structural variations in terms of fibrous structures. Structural variation may be desired as it suggests heterogeneity. However, in practice, too large of a structural variation may not be desirable because it impacts perceived spatial uniformity (McClements & Grossmann, 2022). The SPI and SPI-MBPI samples had a similar trend to PPI samples, which agrees with the similar range of expert fiber scores received by these samples. A unique sample among the similarity analysis was SPI-PPI with 40 wt.% dry matter with a median similarity score of 0.70, very close to the similarity threshold found earlier (0.72). Therefore, from a formulation selection perspective, SPI-PPI with 40 wt.% dry matter may have the most potential of visually mimicking the cooked chicken appearance.

3.5 | General discussions

The Fiberlyzer method has demonstrated its potential as an alternative and automated method to assess fibrousness in HTSC samples.

However, there are some limitations that the image-based Fiberlyzer method carries. First, as shown in Figure 4a, tofu was misidentified to have fibrous structures due to false fiber segmentations. Therefore, suitable samples for the Fiberlyzer method should be limited to meat analogues that are free of surface moisture to minimize interference of light reflection. In addition, a parameter search demonstrated in Section 3.3 may be necessary to identify the best image processing parameters because the Fiberlyzer method relies on a saturation-based segmentation method. Changes of lighting conditions and imaging devices may further impact the segmentation parameters, so calibrations may be needed when implementing the method with a new imaging setup. Lastly, the Fiberlyzer method requires to fold the HTSC sample to expose the inner structure. The folding leads to fracturing of the HTSC sample, making it impossible to assess fibrous structure nondestructively for in-situ measurements.

Despite the mentioned limitations, the Fiberlyzer method can serve as a digital method to replace the conventional expert inspection of visual fibrousness of meat analogues in most of the cases. In addition to the immediate application in the assessment of visual fibrousness, the Fiberlyzer method may empower potential future applications. One potential future application lies in the optimization of formulations and processing conditions for meat analogues. The method can be used to precisely pinpoint differences between the meat products and the analogues. The use of the method can lead to valuable insights on the effect of different ingredients, dry matter contents, temperature, shear rate, and other processing conditions on the visual texture of the products. This information can then be used to optimize and tailor the texture of meat analogues to fit consumer wishes. Additionally, with Fiberlyzer being a rapid method for quantification of visual fibrousness, it could serve as a valuable tool for quality control in meat analogue production industry. For example, deviations and inconsistencies in products are easily detected with the Fiberlyzer method.

Furthermore, the unique fingerprint of visual texture provided by the Fiberlyzer method holds potential to be used in meat analogue research and development. By conducting comparative analyses between meat and meat analogues, a deeper understanding of the differences in textural properties can be achieved. This knowledge can then help to further develop meat analogues that exhibit a closer resemblance to the texture and visual appearance of animal meat. The similarity score in this study was calculated based on cooked chicken as a reference. In the course of time, alternative reference products can be used, such as fish, pork, or beef to allow a broader similarity assessment across meat types.

In the future, the Fiberlyzer method has the potential to bridge the gap between visual fibrousness and mechanical texture properties of meat analogues. Previous studies showed that mechanical anisotropy was not always linked to a visually fibrous macrostructure (Schreuders, Schlangen, Bodnár, et al., 2021). By connecting the computed fiber scores with mechanical analyses, such as tensile testing, the relation between mechanical anisotropy and visual fibrousness can be further understood. Such a clear understanding of fibrous structures helps to develop meat analogues that can best appeal to consumers.

4 | CONCLUSIONS

This study developed and validated an automated visual assessment method (Fiberlyzer) to quantitatively characterize fibrous structures in meat analogues based on image analysis. Fiber shape features were successfully segmented and measured in terms of fiber score (ratio between length and width), fiber area, and number of fiber branches. Among the fiber shape features, fiber score was found to be correlated to expert assessments of fibrousness both at the image ($r^2 = 0.66$) and formulation levels ($r^2 = 0.93$). A similarity analysis was performed to identify the most similar HTSC samples to a reference cooked chicken image, offering a new criterium of selecting visually-mimicking samples for meat analogue applications. The Fiberlyzer method is open-source and simple to be implemented into the current product development routine of meat analogues. Such a digital tool can further contribute to formulation development in the production of meat analogues and enhance the current understanding of visual and textural fibrous structures in meat analogues.

AUTHOR CONTRIBUTIONS

Yizhou Ma: Conceptualization; methodology; software; writing – original draft. **Miek Schlangen:** Conceptualization; methodology; investigation; writing – original draft. **Jelle Potappel:** Methodology; software; investigation; writing – review and editing. **Lu Zhang:** Supervision; writing – review and editing. **Atze Jan van der Goot:** Supervision; writing – review and editing.

ACKNOWLEDGMENTS

The authors would like to thank Aaditya Venkatachalam and Aneesh Chauhan for valuable discussions. The authors extend their appreciation to Merel te Boekhorst for preparing the shear cell samples and images.

FUNDING INFORMATION

This work was partially funded by the Sectorplan Techniek Mechanical Engineering (NWO).

CONFLICT OF INTEREST STATEMENT

The authors declare no conflicts of interest.

DATA AVAILABILITY STATEMENT

The data that support the findings of this study are available from the corresponding author upon reasonable request.

ETHICS STATEMENT

No animals were used in this study. Written informed consent was obtained from all expert survey participants.

ORCID

Yizhou Ma https://orcid.org/0009-0006-3798-8114
Miek Schlangen https://orcid.org/0000-0002-0476-1451
Lu Zhang https://orcid.org/0000-0002-9130-8304

REFERENCES

Barbut, S. (2015). Chapter 16-Evaluating texture and sensory attributes. In *The science of poultry and meat processing* (pp. 603-642). University of Guelph.

Chantanuson, R., Nagamine, S., Kobayashi, T., & Nakagawa, K. (2022). Preparation of soy protein-based food gels and control of fibrous structure and rheological property by freezing. *Food Structure*, *32*-(January), 100258. https://doi.org/10.1016/j.foostr.2022.100258

Dekkers, B. L., Boom, R. M., & van der Goot, A. J. (2018). Structuring processes for meat analogues. *Trends in Food Science & Technology*, *81*, 25–36. https://doi.org/10.1016/j.tifs.2018.08.011

Dekkers, B. L., Nikiforidis, C. V., & van der Goot, A. J. (2016). Shear-induced fibrous structure formation from a pectin/SPI blend. *Innovative Food Science and Emerging Technologies*, *36*, 193–200. https://doi.org/10.1016/j.ifset.2016.07.003

Elzerman, J. E., Hoek, A. C., van Boekel, M. A. J. S., & Luning, P. A. (2011). Consumer acceptance and appropriateness of meat substitutes in a meal context. *Food Quality and Preference*, *22*(3), 233–240. https://doi.org/10.1016/j.foodqual.2010.10.006

Fan, F. H., Ma, Q., Ge, J., Peng, Q. Y., Riley, W. W., & Tang, S. Z. (2013). Prediction of texture characteristics from extrusion food surface images using a computer vision system and artificial neural networks. *Journal of Food Engineering*, *118*(4), 426–433. https://doi.org/10.1016/j.jfoodeng.2013.04.015

Godschalk-Broers, L., Sala, G., & Scholten, E. (2022). Meat analogues: Relating structure to texture and sensory perception. *Food*, *11*(15), 1-31. https://doi.org/10.3390/foods11152227

Grabowska, K. J., Tekidou, S., Boom, R. M., & Van Der Goot, A. (2014). Shear structuring as a new method to make anisotropic structures from soy – Gluten blends. *Food Research International*, *64*, 743–751. https://doi.org/10.1016/j.foodres.2014.08.010

Grabowska, K. J., Zhu, S., Dekkers, B. L., De Ruijter, N. C. A., Gieteling, J., & Van Der Goot, A. J. (2016). Shear-induced structuring as a tool to make anisotropic materials using soy protein concentrate. *Journal of Food Engineering*, *188*, 77–86. https://doi.org/10.1016/j.jfoodeng.2016.05.010

Jia, W., Curubeto, N., Rodríguez-alonso, E., Keppler, J. K., & Van Der, A. J. (2021). Rapeseed protein concentrate as a potential ingredient for meat analogues. *Innovative Food Science and Emerging Technologies*, *72*(July), 102758. https://doi.org/10.1016/j.ifset.2021.102758

Krintiras, G. A., Göbel, J., Van Der Goot, A. J., & Stefanidis, G. D. (2015). Production of structured soy-based meat analogues using simple shear and heat in a Couette Cell. *Journal of Food Engineering*, *160*, 34–41. https://doi.org/10.1016/j.jfoodeng.2015.02.015

Kyriakopoulou, K., Dekkers, B., & van der Goot, A. J. (2019). Plant-based meat analogues. In *Sustainable meat production and processing*. Elsevier Inc. https://doi.org/10.1016/B978-0-12-814874-7.00006-7

Ma, Y., Potappel, J., Chauhan, A., Schutyser, M. A. I., Boom, R. M., & Zhang, L. (2023). Improving 3D food printing performance using computer vision and feedforward nozzle motion control. *Journal of Food Engineering*, *339*, 111277. https://doi.org/10.1016/j.jfoodeng.2022.111277

Ma, Y., Potappel, J., Schutyser, M. A. I., Boom, R. M., & Zhang, L. (2023). Quantitative analysis of 3D food printing layer extrusion accuracy: Contextualizing automated image analysis with human evaluations: Quantifying 3D food printing accuracy. *Current Research in Food Science*, *6*(February), 100511. https://doi.org/10.1016/j.crfs.2023.100511

Marlow, P. J., Gegenfurtner, K. R., & Anderson, B. L. (2022). The role of color in the perception of three-dimensional shape. *Current Biology*, *32*(6), 1387–1394.e3. https://doi.org/10.1016/j.cub.2022.01.026

McClements, D. J., & Grossmann, L. (2022). *Next-generation plant-based foods design, production, and properties*. Springer.

Mcclements, D. J., Weiss, J., Kinchla, A. J., Nolden, A. A., & Grossmann, L. (2021). Methods for testing the quality attributes of plant-based foods: Meat- and processed-meat analogs. 1–30.

Michel, F., Hartmann, C., & Siegrist, M. (2021). Consumer's associations, perceptions and acceptance of meat and plant-based meat alternatives. *Food Quality and Preference*, *87*(August 2020), 104063. https://doi.org/10.1016/j.foodqual.2020.104063

Nieuwland, M., Heijnis, W., van der Goot, A. J., & Hamoen, R. (2023). XRT for visualizing microstructure of extruded meat replacers. *Current Research in Food Science*, *6*(December 2022), 100457. https://doi.org/10.1016/j.crfs.2023.100457

Osen, R., Toelstede, S., Wild, F., Eisner, P., & Schweiggert-Weisz, U. (2014). High moisture extrusion cooking of pea protein isolates: Raw material characteristics, extruder responses, and texture properties. *Journal of Food Engineering*, *127*, 67–74. https://doi.org/10.1016/j.jfoodeng.2013.11.023

Ranasinghesagara, J., Hsieh, F., & Yao, G. (2005). An image processing method for quantifying fiber formation in meat analogs under high moisture extrusion. *Food Engineering and Physical Properties*, *70*(8), 450–454.

Ranasinghesagara, J., Hsieh, F., & Yao, G. (2006). A photon migration method for characterizing fiber formation in meat analogs. *Journal of Food Science*, *71*(5), E227–E231. https://doi.org/10.1111/j.1750-3841.2006.00038.x

Ranasinghesagara, J., Hsieh, F.-H., Huff, H., & Yao, G. (2009). Laser scanning system for real-time mapping of fiber formations in meat. *Food Engineering and Phyiscal Properties*, *74*(2), E39–E45. https://doi.org/10.1111/j.1750-3841.2008.01032.x

Ridout, M. S., & Linkie, M. (2009). Estimating overlap of daily activity patterns from camera trap data. *Journal of Agricultural, Biological, and Environmental Statistics*, *14*(3), 322–337. https://doi.org/10.1198/jabes.2009.08038

Samard, S., & Ryu, G. H. (2019). Physicochemical and functional characteristics of plant protein-based meat analogs. *Journal of Food Processing and Preservation*, *43*(10), 1–11. https://doi.org/10.1111/jfpp.14123

Schlangen, M., Ribberink, M. A., Taghian, S., Sagis, L. M. C., & van der Goot, A. J. (2023). Mechanical and rheological effects of transglutaminase treatment on dense plant protein blends. *Food Hydrocolloids*, *136*-(Part A), 108261. https://doi.org/10.1016/j.foodhyd.2022.108261

Schreuders, F. K. G., Dekkers, B. L., Bodnár, I., Erni, P., Boom, R. M., & van der Goot, A. J. (2019). Comparing structuring potential of pea and soy protein with gluten for meat analogue preparation. *Journal of Food Engineering*, *261*(April), 32–39. https://doi.org/10.1016/j.jfoodeng.2019.04.022

Schreuders, F. K. G., Schlangen, M., Bodnár, I., Erni, P., Boom, R. M., & van der Goot, A. J. (2021). Structure formation and non-linear rheology of blends of plant proteins with pectin and cellulose. *Food Hydrocolloids*, *124*(September 2021), 107327. https://doi.org/10.1016/j.foodhyd.2021.107327

Schreuders, F. K. G., Schlangen, M., Kyriakopoulou, K., Boom, R. M., & van der Goot, A. J. (2021). Texture methods for evaluating meat and meat analogue structures: A review. *Food Control*, *127*(April), 108103. https://doi.org/10.1016/j.foodcont.2021.108103

Sharma, R., Kumar, M., & Alam, M. S. (2021). Image processing techniques to estimate weight and morphological parameters for selected wheat refractions. *Scientific Reports*, *11*(1), 1–12. https://doi.org/10.1038/s41598-021-00081-4

Taheri-Garavand, A., Fatahi, S., Omid, M., & Makino, Y. (2019). Meat quality evaluation based on computer vision technique: A review. *Meat*

Science, *156*(December 2018), 183–195. https://doi.org/10.1016/j.meatsci.2019.06.002

van der Sman, R. G. M., & van der Goot, A. J. (2023). Hypotheses concerning structuring of extruded meat analogs. *Current Research in Food Science*, *6*(April), 100510. https://doi.org/10.1016/j.crfs.2023.100510

Webb, D., Dogan, H., & Li, Y. (2023). Physico-chemical properties and texturization of pea, wheat and soy proteins using extrusion and their application in plant-based meat. *Food*, *12*(8), 1-25. https://doi.org/10.3390/foods12081586

Wittek, P., Karbstein, H. P., & Emin, M. A. (2021). Blending proteins in high moisture extrusion to design meat analogues: Rheological properties, morphology development and product properties. *Food*, *10*(7), 1-18. https://doi.org/10.3390/foods10071509

Zapotoczny, P., Zielinska, M., & Nita, Z. (2008). Application of image analysis for the varietal classification of barley::Morphological features. *Journal of Cereal Science*, *48*(1), 104–110. https://doi.org/10.1016/j.jcs.2007.08.006

SUPPORTING INFORMATION

Additional supporting information can be found online in the Supporting Information section at the end of this article.

How to cite this article: Ma, Y., Schlangen, M., Potappel, J., Zhang, L., & van der Goot, A. J. (2023). Quantitative characterizations of visual fibrousness in meat analogues using automated image analysis. *Journal of Texture Studies*, 1–12. https://doi.org/10.1111/jtxs.12806